EUSAR 2021 . ISBN 978-3-8007-5457-1 / ISSN 2197-4403 . ©VDE VERLAG GMBH . Berlin . Offenbach

Polarimetric Scattering based Support GLRT for Detection of Permanent Scatterers

H. Aghababaei[a], G. Ferraioli[b], A. Budillon[c], V. Pascazio[c], G. Schirinzi[c]
[a] Faculty of Geo-Information Science and Earth Observation (ITC), Department of Earth Observation Science (EOS), University of Twente, Enschede, the Netherlands.
[b] Dipartimento di Ingegneria, Università degli Studi di Napoli "Parthenope," Napoli, Italy
[c] Dipartimento di Scienze e Tecnologie, Università degli Studi di Napoli "Parthenope", Napoli, Italy

Abstract

This paper deals with the characterization of permanent scatterers in polarimetric synthetic aperture radar (SAR) images of urban environment. Along this line, a scattering property based generalized likelihood ratio (GLRT) test for detection of permanent single and double scatterers, called scat-sup GLRT, is proposed. The method uses polarimetric information within the test, which allows further improvement in detection performance and identification of backscattering mechanisms of the permanent scatterers (PSs). Hence allowing identification and classification of PSs. The proposed framework is evaluated using satellite polarimetric multi-baseline data sets and compared with existing PS detection using SAR tomography framework.

1 Introduction

Polarimetric synthetic aperture radar (SAR) remote sensing has been used as a powerful tool for monitoring of the Earth's surface, particularly in producing the land-use and land-cover classification map of complex urban environment [1]. Generally, over the complex urban scenario, different scattering mechanisms including odd-bounce scattering from roofs and from the ground, double-bounce scattering due to wall-ground reflections, and volumetric scattering over vegetated urban areas may fall into one single SAR resolution cell due to the geometric distortion or layover phenomena. Such a problem represents a severe limitation for the characterization of the pixels using the conventional PolSAR image processing which forces to perform the analysis in azimuth-range two-dimensional space.

To the aim of multi-dimensional target scattering identification, the 3D image reconstruction of urban environment with above-mentioned backscattering mechanisms is required. SAR tomography (TomoSAR) with resolution capability in the height and velocity dimensions is a natural solution to reconstruct backscattering from urban environment. This multi-dimensional imaging technique is today widely exploited in remote sensing of complex urban environment [2-5]. Along this, availability of polarization information can boost the synthesizing performance and allows describing the electromagnetic behavior of illuminated objects that presented in a resolution cell but at different elevations.

One important aspect of TomoSAR focusing using space-borne data set is related to the identification of permanent scatterers (PSs). For the application of multi-dimensional imaging, the detection problem becomes a key issue. In particular, we are interested in increasing the number of monitored scatterers, but at the same time, it is mandatory to keep low the probability of signal mis-interpretation. This issue can be approached by the detection methods that allow controlling the false alarm rate (FAR) such as Generalized Likelihood Ratio Test (GLRT).

In literature, to address the problem of accurate estimation of true scatterers, some detection methods, such as generalized-likelihood ratio test (GLRT) [6], support estimation GLRT [7] have been employed. These schemes were shown to be a constant false alarm rate (CFAR) test. Moreover, those were a kind of single look detectors, which allows preserving full spatial azimuth-range resolution, while the main concern might be the number of detected scatterers in the scene. Most recently, the drawback of SNR in the detection process has been mitigated by appropriate multi-looking in [8]. Moreover, reference [9] employed polarimetric data set in order to improve detection process by increasing the length of observation vector.

In this regard, we propose the extension of GLRT to polarimetric data set. Our proposed approach is different from [9], in which the polarimetric information is employed inside the detection test in order to increase the performance of the method. We investigate the benefits offered by the usage of multiple polarization observations. Generally, the aim is to derive a simple and effective detection scheme able to improve the detection capability over urban environments. To deal with the areas characterized by a low SNR, multi-looked polarimetric GLRT is adapted. The peculiarity of our proposed approach is related to employment of polarimetric information in PS detection, which not only improve the detection performance but also allows the classification and characterization of permanent scatterers. Hence, the proposed approach can be considered as a first attempt for PSs classification besides extracting their parameter related to the displacement. In summary, the outcomes of this study paves a comprehension on how space-borne polarimetric data can be employed for the fully characterization of PSs.

2 Polarimetric TomoSAR Signal Model

For a specific azimuth-range resolution cell in the polarimetric SAR image that contains L scatterers located at different elevations, the polarimetric data vector with p polarization channels measured by a multi-baseline TomoSAR configuration over N acquisition $\mathbf{y}\in\mathbb{C}^{N\times 1}$ can be represented by [10]:

$$\mathbf{y}_{\mathrm{p}}(l)=\sum \mathbf{a}(\boldsymbol{\theta}_i,\mathbf{k}_i)\gamma_i(l)+n(l) \tag{1}$$

where $\mathbf{y_p}(l)=[\ \mathbf{y_1}(l)^{\mathrm{T}}\ \ \mathbf{y_2}(l)^{\mathrm{T}}\ \ \ldots.\ \mathbf{y_p}(l)^{\mathrm{T}}\ ]^{\mathrm{T}}\in\mathbb{C}^{Np\times l}$ is a vector contains p multi-baseline data $\mathbf{y}_i(l)\in\mathbb{C}^{N\times l}$ in p different polarization channels. γ is the spectral distribution with l realizations of the signal acquisition, and $\mathbf{a}(\boldsymbol{\theta}_i,\mathbf{k}_i)$ indicating the polarimetric steering vector related to the i^{th} scatterer in the resolution cell. Note that $\boldsymbol{\theta}$ represents the elevation direction in the 3D case, or elevation and deformation velocity in 4D case, or elevation, deformation velocity, and thermal dilation in 5D case, while $\mathbf{k}_i$ is the polarimetric scattering pattern of i^{th} scatterer. Finally, $\mathbf{n}$ is the complex additive noise with Gaussian distribution, zero mean and standard deviation of σ_n^2.

Then, the covariance matrix of observed polarimetric signal (1) is generally given by $\mathrm{R}=E\{\mathbf{y_p}\mathbf{y_p}^{\dagger}\}$, where E and † are the expectation and Hermitian operators, respectively.

3 Scat-Sup GLRT

The goal of the proposed detector is to separate different scatterers interfering in the same pixel and correctly locate them. We assume at most two different scatterers in the same azimuth-range cell and sparseness in the elevation direction. Then the detection problem can be formulated as:

$$\begin{aligned}
&\mathrm{H}_0:\ \ \mathbf{y}_p(l)=\mathbf{n}(l)\\
&\mathrm{H}_1:\ \ \mathbf{y}_p(l)=\mathbf{a}(\boldsymbol{\theta}_1,\mathbf{k}_1)\gamma_1(l)+\mathbf{n}(l)\\
&\mathrm{H}_2:\ \ \mathbf{y}_p(l)=\sum_{i=1}^{2}\mathbf{a}(\boldsymbol{\theta}_1,\mathbf{k}_1)\gamma_1(l)+\mathbf{n}(l)
\end{aligned} \tag{2}$$

Generally, the proposed multi-look GLRT for the binary hypotheses test (H_m, H_n) can be written by:

$$\frac{\max\limits_{\boldsymbol{\Theta}_m,\mathbf{K}_m} f(\mathbf{y}_{\mathrm{p}}(1),\ldots.\mathbf{y}_{\mathrm{p}}(L),\boldsymbol{\Theta}_m,\mathbf{K}_m\mid \mathrm{H}_m)}{\max\limits_{\boldsymbol{\Theta}_n,\mathbf{K}_n} f(\mathbf{y}_{\mathrm{p}}(1),\ldots.\mathbf{y}_{\mathrm{p}}(L),\boldsymbol{\Theta}_n,\mathbf{K}_n\mid \mathrm{H}_n)} \tag{3}$$

where f is the joint pdf of the looks, and $\boldsymbol{\Theta}$ is ensemble of all unknown parameters, *i.e.* $\boldsymbol{\Theta}_{\mathrm{n}}=[\boldsymbol{\theta}_1\ \ \boldsymbol{\theta}_2\ \ldots\ldots\ \boldsymbol{\theta}_{\mathrm{n}}]$. Moreover, $\mathbf{K}$ denotes the unknown polarization pattern of the scatterers. i.e. $\mathbf{K}_{\mathrm{n}}=[\mathbf{k}_1\ \mathbf{k}_2\ \ldots..\ \mathbf{k}_{\mathrm{n}}]$. In this study, we assumed the two scatterers at most per each resolution cell. Hence, it can be proved that the first stage of the proposed multi-look scattering based support GLRT acts the decision rule of presence or absence of scatterers as [11]:

$$\begin{aligned}
&\frac{\lambda_{\max}\left(\mathbf{B}^{\dagger}(\boldsymbol{\Theta}_2)\,\hat{\mathbf{R}}_{\mathrm{p}}\,\mathbf{B}(\boldsymbol{\Theta}_2)\right)}{trace\left(\hat{\mathbf{R}}_{\mathrm{p}}\right)}\ \underset{\bar{H}_0}{\overset{H_0}{\gtrless}}\ th\\
&\mathbf{B}(\boldsymbol{\Theta}_2)=\left[\mathbf{I}\otimes\mathbf{a}(\boldsymbol{\theta}_1)\ \ \ \mathbf{I}\otimes\mathbf{a}(\boldsymbol{\theta}_2)\right]
\end{aligned} \tag{4}$$

where $\bar{H}_0$ is the complement of H_0, and $\mathbf{I}$ is an N×P identify matrix. It can be proved that the second stage of the proposed scattering based support GLRT, operates the decision according to the rule of presence of single or double scatterers (H_1, H_2), is representable as:

$$\frac{1-\dfrac{\lambda_{\max}\left(\mathbf{B}^{\dagger}(\boldsymbol{\Theta}_2)\hat{\mathbf{R}}_{\mathrm{p}}\mathbf{B}(\boldsymbol{\Theta}_2)\right)}{\mathrm{trace}\{\hat{\mathbf{R}}_{\mathrm{p}}\}}}{1-\dfrac{\lambda_{\max}\left(\mathbf{B}^{\dagger}(\boldsymbol{\Theta}_1)\hat{\mathbf{R}}_{\mathrm{p}}\mathbf{B}(\boldsymbol{\Theta}_1)\right)}{\mathrm{trace}\{\hat{\mathbf{R}}_{\mathrm{p}}\}}}\ \underset{H1}{\overset{H_2}{\gtrless}}\ th \tag{5}$$

In (5), $\hat{\mathbf{R}}_{\mathbf{p}}$ represents the estimated multi-baseline polarimetric sample covariance matrix. The above theoretical formulation shows that by eigenvalue decomposition the proposed tests can be written independent of the parameters related to the polarimetric scattering pattern and they are only the function of TomoSAR unknown parameter i.e. $\boldsymbol{\theta}$. Moreover, $\boldsymbol{\theta}_1$ and $\boldsymbol{\theta}_2$ in (4) and (5) can be obtained by MLE approach, and the fast implementation allows decoupled MLEs as:

$$\begin{aligned}
\hat{\boldsymbol{\theta}}_1&=\max_{\boldsymbol{\theta}_1}\left(\lambda_{\max}\left(\mathbf{B}^{\dagger}(\boldsymbol{\theta}_1)\hat{\mathbf{R}}_{\mathbf{p}}\mathbf{B}(\boldsymbol{\theta}_1)\right)\right)\\
\hat{\boldsymbol{\theta}}_2&=\max_{\boldsymbol{\theta}_2}\left(\lambda_{\max}\left(\mathbf{B}^{\dagger}(\hat{\boldsymbol{\theta}}_1,\boldsymbol{\theta}_2)\hat{\mathbf{R}}_{\mathbf{p}}\mathbf{B}(\hat{\boldsymbol{\theta}}_1,\boldsymbol{\theta}_2)\right)\right)
\end{aligned} \tag{6}$$

The main peculiarity of the proposed detection test is related to the identification of the scattering mechanism. Once the PSs are detected from the above equations, their unitary polarimetric scattering type can be represented by the eigenvector $\mathbf{e}_{\max}$ corresponding to the maximum eigenvalue of the following Hermitian matrix:

$$\left(\mathbf{B}^{\dagger}(\boldsymbol{\theta}_i)\hat{\mathbf{R}}_{\mathbf{p}}\mathbf{B}(\boldsymbol{\theta}_i)\right)\mathbf{e}_{\max}=\lambda_{\max}\mathbf{e}_{\max} \tag{7}$$

It can be understood that $\mathbf{e}_{\max}$ is optimal polarization pattern with respect to the beamforming criterion.

4 Numerical Experiments

A tomographic data set is simulated by exploiting the system parameters of TerraSAR-X stack of N= 22 dual-polarization p=2 images, with wavelength λ=0.031 m, incident angle around 28°, and range distance of 579 km.

The data are simulated with presence of single scatterer with the parameter vector $\boldsymbol{\theta}_1=[s_1,v_1]^{\mathrm{T}}=[0,0]^{\mathrm{T}}$. The additional scatterer with $\boldsymbol{\theta}_2=[\mathrm{s1},v_2]^{\mathrm{T}}=[1.5\ ru,\ 0]^{\mathrm{T}}$ is simulated for the case of double scatterer, where ru is the Rayleigh resolution [12]. The total signal power is defined by $\sigma_s=\sigma_{s1}+\sigma_{s2}$, where σ_{si} is the polarimetric signal power of i^{th} scatterer and $\sigma_{s2}/\sigma_{s1}=0.8$.

In the analyses, the probabilities of detection (PD) and false alarm (PFA) are evaluated by resorting to Monte

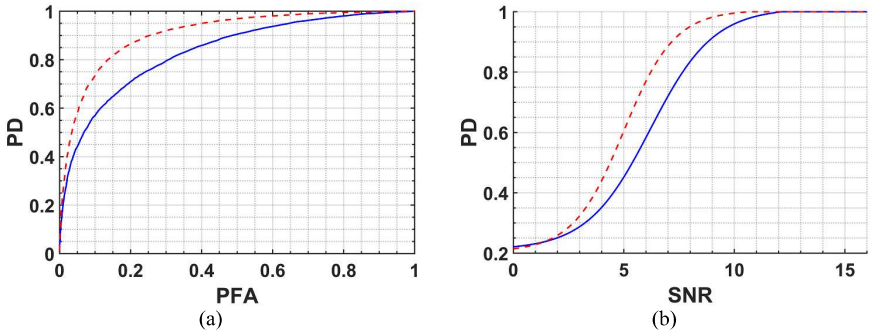

Fig. 1. Performance assessment of the proposed scat-sup GLRT (red-dash profiles) and existing support GLRT [9] (blue profiles) for discrimination of single and double scatterers. **(a)** ROC curve, **(b)** plot of PD versus different SNR values.

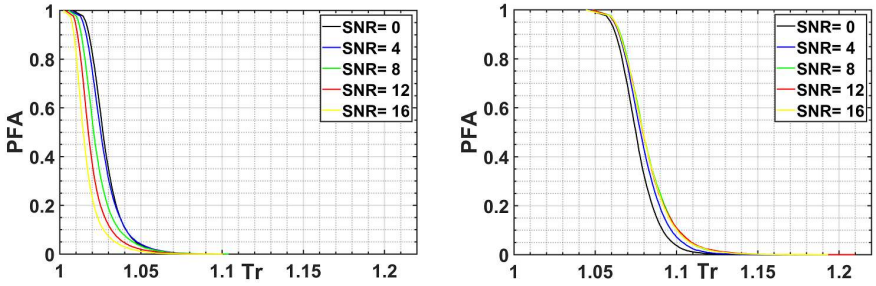

Fig. 2. Thresholds of second stage with respect to PFA in different SNR **(a)** The proposed scat-sup GLRT **(b)** conventional support GLRT [9].

Carlo techniques over 10^5 realizations of simulated data. Moreover, the parameter space were uniformly discretized over the interval of [-4*r*u, 4*ru*] in both elevation and velocity domains.

The effectiveness of the proposed approach is compared with multi-looked version of the techniques presented in [9]. Both of the employed methods are evaluated in the same way with respect to the detection of double scatterers. For testing the detector capability of discriminating the two superimposed scatterers, the ROC curves are shown in Fig. 1(a), for the simulated data with fixed SNR = 6 dB. Moreover, the extensive experiments are reported by giving the PD of the detectors with respect to different SNR values in Fig. 1(b). As expected, by increasing the SNR the probability of detection is improved for both detector. However, in this case, as can be verified from the plots, the proposed detector (red dash curve) significantly outperforms the conventional support GLRT (blue curve). This improvement is mainly related to the fact that the proposed method is based on scattering pattern of polarimetric covariance matrices of the PSs, while the conventional support GLRT employs the reflectivity of the PSs.

Moreover, the behaviors of the thresholds in the second stage of the methods with respect to different SNRs are plotted in Fig. 2. The second threshold is exploited for discriminating between the presence of one and two scatterers, and its independence to the SNR is the main point in PS TomoSAR detection. The given profiles confirm that the thresholds do not change considerably with variation of SNR.

5 Experimental Results

For the evaluation of the method, a set of Sentinel-1 data set composed by 65 dual-polarization images acquired between 18 February 2017 and 27 May 2019, were employed. In particular, the considered detection approaches were used to reconstruct the single and double scatterers of the international Tehran building with 162 m height. The building height is about twice bigger than the Rayleigh resolution.

From the implementation of the proposed method and existing support GLRT [9], the detected single and double scatterers are transformed into the optical 3D Google Earth image of the building. Fig. 3 reports the elevation of the scatterers estimated using the employed approaches, as can be seen more scatterers are detected by proposed approach. In the figure, the color is changing from blue to red by passing from the scatterers on the ground to the ones on top of the building.

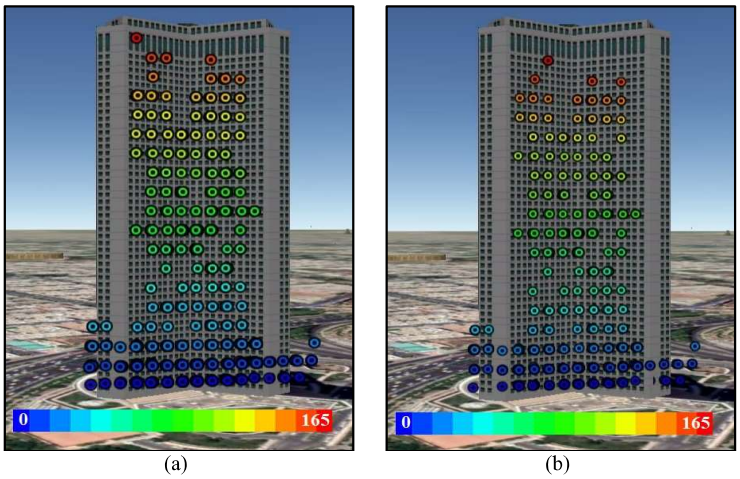

(a) (b)

Fig. 3. The detected scatterers reported on the optical images. (a) The proposed approach. (b) Existing support GLRT [9]

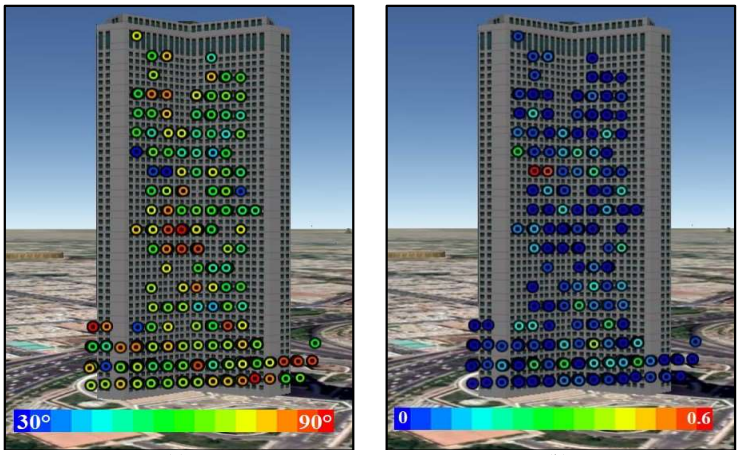

(a) (b)

Fig. 4. Estimated polarimetric feature of the detected scatterers using the proposed scattering support GLRT. **(a)** Scattering angle ($\bar{\alpha}$) and **(b)** entropy.

As noted before, in addition to the efficiency of the proposed method in detection process, the other particular aspect of proposed method is related to the identification of the backscattering mechanisms of the detected PSs. To analyze the backscattering properties of the detected scatterers using the proposed scattering based support GLRT, their scattering angle and entropy are reported into the 3D Google Earth image shown in Fig. 4. The range of estimated $\bar{\alpha}$ angle for the scatterers is up to 30˚, while the entropy does not exceed from 0.56. Transferring the computed polarimetric features ($\bar{\alpha}$,H) into the conventional H/α plane which is not reported here for sake of brevity, shows that most of the scatterers are situated in zone 7 indicating dihedral reflectors.

It should be noted that such a polarimetric features in Fig. 4 can only be obtained using the proposed detection and identification approach, where allows to classify the permanent scatterers beside identification of their elevation/velocity parameters.

In the conference, more experimental results using high-resolution Terrasar-X images will be provided.

Literature

[1] J.-S. Lee and E. Pottier, *Polarimetric radar imaging: from basics to applications*. CRC press, 2009.

[2] H. Aghababaee, A. Budillon, G. Ferraioli, V. Pascazio, and G. Schirinzi, "Full 3D DEM Generation in Urban Area By Improving Estimation from SAR Tomography," in *IGARSS 2018 - 2018 IEEE International Geoscience and Remote Sensing Symposium*, 2018, pp. 6087-6090.

[3] H. Aghababaei, A. Budillon, G. Ferraioli, A. C. Johnsy, V. Pascazic, and G. Schirinzi, "Multiple Scatterers Detection Based on Signal Correlation Eploitation in Urban Sar Tomography," in *IGARSS 2018 - 2018 IEEE International Geoscience and Remote Sensing Symposium*, 2018, pp. 8691-8694.

[4] G. Fornaro and F. Serafino, "Imaging of Single and Double Scatterers in Urban Areas via SAR Tomography," *IEEE Transactions on Geoscience and Remote Sensing*, vol. 44, no. 12, pp. 3497-3505, 2006.

[5] X. X. Zhu and R. Bamler, "Demonstration of Super-Resolution for Tomographic SAR Imag-

ing in Urban Environment," *IEEE Transactions on Geoscience and Remote Sensing,* vol. 50, no. 8, pp. 3150-3157, 2012.

[6] A. Pauciullo, D. Reale, A. D. Maio, and G. Fornaro, "Detection of Double Scatterers in SAR Tomography," *IEEE Transactions on Geoscience and Remote Sensing,* vol. 50, no. 9, pp. 3567-3586, 2012.

[7] A. Budillon and G. Schirinzi, "GLRT Based on Support Estimation for Multiple Scatterers Detection in SAR Tomography," *IEEE Journal of Selected Topics in Applied Earth Observations and Remote Sensing,* vol. 9, no. 3, pp. 1086-1094, 2016.

[8] A. Pauciullo, D. Reale, W. Franzé, and G. Fornaro, "Multi-Look in GLRT-Based Detection of Single and Double Persistent Scatterers," *IEEE Transactions on Geoscience and Remote Sensing,* vol. 56, no. 9, pp. 5125-5137, 2018.

[9] A. Budillon, A. C. Johnsy, and G. Schirinzi, "Urban Tomographic Imaging Using Polarimetric SAR Data," *Remote Sensing,* vol. 11, no. 2, p. 132, 2019.

[10] Y. Huang, L. Ferro-Famil, and A. Reigber, "Under-Foliage Object Imaging Using SAR Tomography and Polarimetric Spectral Estimators," *IEEE Transactions on Geoscience and Remote Sensing,* vol. 50, no. 6, pp. 2213-2225, 2012.

[11] H. Aghababaee, A. Budillon, G. Ferraioli, V. Pascazio, and G. Schirinzi, "3D target scattering classification using full-raank polarimetruc tomographic SAR focusing," in *IGARSS 2019 IEEE International Geoscience and Remote Sensing Symposium*, 2019, pp. 6087-6090: IEEE.

[12] G. Fornaro, F. Serafino, and F. Soldovieri, "Three-dimensional focusing with multipass SAR data," *IEEE Transactions on Geoscience and Remote Sensing,* vol. 41, no. 3, pp. 507-517, 2003.